

ICM11

Vacuum Oxy-nitrocarburization of Ultra Fine Electrolytic Iron

M.P. Nikolova^{a*}, P.S. Danev^a, I.D. Dermendjiev^a, D.D. Gospodinov^a

^aUniversity of Ruse, 8 Studentska Str., 7017 Ruse, Bulgaria

Abstract

Samples of Armco iron with electrolytic Fe coating were hardened by vacuum oxy-nitrocarburizing at low temperature. The carbon amount (CO₂) in the nitriding atmosphere (NH₃) was 10 vol. % at a pressure of 8.10⁴ Pa and the process time was 7 h. The influence of the structural difference on the depth profile, hardness distribution and X-ray diffraction pattern of the oxy-nitrocarburized specimens were performed. The indicated parameters of the modified surface of electrolyte-precipitated Fe were compared to those of re-crystallized at low-temperature and fully annealed in vacuum and oxy-nitrocarburized specimens. The results confirmed formation of γ' - and ε -phases in the compound layer in all samples in different proportions. A significant alteration/ difference in the phase distribution between the electrolyte-precipitated Fe layer and the substrate was demonstrated due to the ultra fine grained structure of the iron.

© 2011 Published by Elsevier Ltd. Selection and/or peer-review under responsibility of ICM11

Keywords: thermo-chemical treatment; compound zone; diffusion zone; hardness profile; X-ray diffraction

1. Introduction

There are different gaseous ferrite nitrocarburizing methods among which are the low pressure processes in NH₃ and CO₂ mixture atmosphere. At temperature lower than 590°C the carbon solubility in α -Fe is u/insignificant and its/carbon atoms participates only in ε -Fe_{2.3}(N,C) formation. The CO₂ containing gas phase has a comparatively high oxygen potential and the oxygen atoms catalysis the ε -Fe_{2.3}(N,C) formation [1]. At low pressure conditions oxygen contributes in adherent nitrocarburized layers formation [2]. The structure of the layers depends on process conditions, gas composition and the substrate specific features [3]. It is established that gaseous oxy-nitrocarburizing increases surface

* Corresponding author. Tel.: +359888785133
E-mail address: mpnikolova@uni-ruse.bg (M.P. Nikolova)

hardness and wear resistance, enhances fatigue strength and corrosion resistance of inexpensive non-alloyed or low-alloy steels. The aim of the study is to determine the structural and hardness differences of vacuum oxy-nitrocarburized layers formed on metallurgically and galvanically obtained iron substrate in NH_3 and CO_2 containing gas phase.

2. Experimental details

Samples of an Armco iron with thickness about 10 mm and chemical composition (“SPECTRON” quantometer) according to listed in Table 1 are used as substrates for electrolytic Fe deposition and oxy-nitrocarburizing. Before electroplating, the samples were electrochemically cleaned...

{ Samples of an Armco iron with an electrolytic iron coating (overall thickness about 10 mm) are used for the metallographic study, X-ray diffraction analysis and hardness measurements in depth of the oxy-nitrocarburized layer. The chemical composition of Armco and electrolytic Fe obtained/analysed using “SPECTRON” quantometer is shown in Table 1. }

Table 1. Chemical composition of Armco and electrolytic iron (wt %)

Element	C, %	Si, %	Mn, %	Cr, %	Mo, %	Ni, %	Co, %	Cu, %	P, %	S, %	Fe, %
Armco Fe	0,020	0,130	0,139	0,033	0,002	0,073	0,008	0,090	0,007	0,020	Bal.
Electrolytic Fe	0,000	0,015	0,003	0,004	0,002	0,028	0,015	0,040	0,006	0,002	Bal.

The Armco samples were used as anodes/ electrochemically cleaned for 20-30 s in 30% water solution of H_2SO_4 and current density of $D_A \sim 100 \text{ A/dm}^2$ in order to improve the adhesion. The electrolytic Fe coating was obtained in water solution of $\text{FeCl}_2 \cdot 4\text{H}_2\text{O}$ (30 g/l) turned sour/acidified by HCl up to $\text{pH} = 1 - 1,2$. The electrolysis is carried out at $80 \pm 2^\circ\text{C}$, current density of $D_K = 10 \text{ A/dm}^2$ and a run time of 8h. Steel strips (DIN - R St 37-2) were used as anodes. Afterwards two of the samples were vacuum annealed for 1h under a pressure of 200 Pa at 600°C and 950°C . The chemical composition of the electrolytic Fe layer is shown in table 1.

The vacuum oxy-nitrocarburizing was carried out in industrial equipment for 7 hours at 550°C in NH_3 and CO_2 atmosphere. The pressure in the vacuum chamber has been $8 \cdot 10^4 \text{ Pa}$ for the first 5 hours and $1 \cdot 10^5 \text{ Pa}$ during the last 2 hours [4]. The surface hardness was measured by a mobile ‘Krautkramer’ Vickers tester (before and after the nitrocarburizing) under a load of 1 kg. The microhardness was measured under a load of 0,05 kg according to a chess-board order 4...5 times for each sample. The microstructure was etched by 4%-solution of HNO_3 in ethyl alcohol (Nital) and Murakami reagent. X-ray diffractometer URD 6 using $\text{FeK}\alpha$ radiation was used to determine the phase composition. $\epsilon\text{-Fe}_{2-3}(\text{N,C})$ lattice parameters were determined according to [5]. The structural characterizations before and after modification of the layers were investigated using Olympus BX41M optical microscopy.

3. Results and Discussions

3.1 Microstructure

Fig. 1 displays the microstructures of founded Armco Fe, electrolytic Fe and vacuum annealed electrolytic Fe at 600°C and 950°C respectively. The Armco Fe ferrite microstructure with Fe_3C at the grains’ boundaries and rarely in the grains (fig. 1a) is comparatively coarse (average $20 \mu\text{m}$ grain size). Unlike, the galvanically received Fe (fig. 1b) has a totally/entirely different structure and properties. The electrolytic Fe is obtained at a low density asymmetric current in the bath (see 2). In/at this condition, the

ferrite nuclei are small because of the lower Fe-ions' mobility in low voltage. The supply ions rate is lower than the ferrite nuclei growth. As a result the density current is redistributed over nuclei-free areas. In restrain growth conditions, oxygen and other surface active components passivate the nuclei. Ions such as Ni, Mn, especially Cu from the anodes and $\text{Fe}_x(\text{OH})$ from the solution also precipitate/incorporate in the nuclei, thus increases the surface strain which is a precondition for development of micro- and submicrocracks. So, the electrolyte Fe presents a porous and tense aggregates of small, slightly bounded crystals which mounted perpendicularly to the substrate thus decreasing the surface free energy of the growing up layer.

The vacuum annealed electrolytic Fe at 600°C (fig. 1c) contains re-crystallized ferrite grains located predominantly near to the surface where the microstrains of the ultra fine grains are higher. The fully vacuum annealed electrolytic Fe structure (fig.1d) shows that coarse ferrite grains substitute the ultra fine structure. Globular fine phases of into oxides are present in the α -Fe grains.

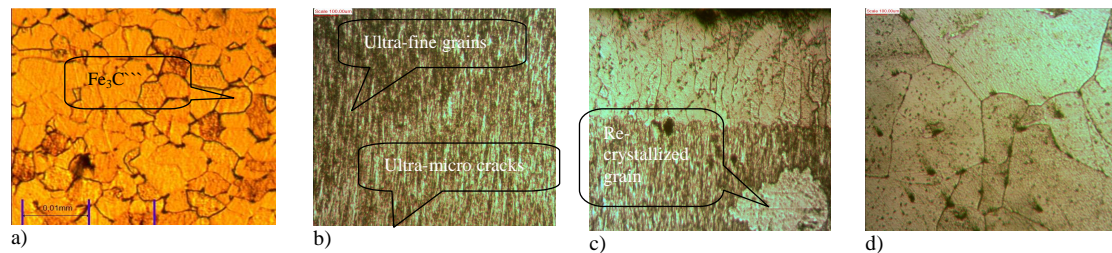


Fig.1 Microstructure images of the iron before oxy-nitrocarburizing: a) Armco iron (200x, etched in Nital); b) untreated electrolytic iron (500x, Nital); c) vacuum annealed electrolytic iron at 600°C. (500x, Nital); d) vacuum annealed electrolytic iron at 950°C (500x, Nital).

Fig.2 represents the microstructure of the oxy-nitrocarburized layers formed on the different substrates. The distances of N and C diffusion in ultra fine grained Fe are less than that in the annealed samples as seen on fig.2a. The gas-solid interaction rate depends on the adsorption rate and the latter has a constant quantity at a constant temperature. The nascent atoms retard the diffusion rate when they reach up the substrate grains. The diffusion there runs across the α -Fe grains and the boundaries. The Armco γ - Fe_4N needles are coarse and consolidated deeper in the substrate. Darker colored ε - $\text{Fe}_{2,3}(\text{N},\text{C})$ are seen mainly near to the surface, at the grater microcracks and the electrolyte-Armco Fe boundary. The initial C enrichment precedes compound layer formation during gas nitrocarburizing of Fe and steel [6]. As a smaller molecule, CO_2 is absorbed through the pores of the layer. A carbon concentration gradient in depth probably renders the N penetration because C increases the nitrogen activity. This fact corresponds with the slower rate of compound layer formation. The latter seems comparatively thin and torn to pieces. The faster diffusion in the electrolytic Fe renders surface limited concentration for dense compound layer formation. At the same time, N and C nascent atoms gather the electrolyte-Armco Fe boundary where a secondary adjacent compound layer could be formed [7,8]. Some re-crystallized α grains are present in the electrolyte Fe layer after oxy-nitrocarburizing, whereas they are absent before the saturation. A possible reason for this is the formation of $\text{Fe}_\alpha(\text{N})$ or $\text{Fe}_\alpha(\text{N},\text{C})$. Hence the process time and temperature are enough for primary re-crystallization to begin especially in microstrained zones.

Carbon enriched areas in vacuum annealed at 600°C electrolyte Fe (fig. 2b) are closely adjacent to the compound layer where carbonitrides in the recrystallized grains are very fine. The compound layer is thicker than in the untreated oxy-nitrocarburized electrolytic Fe and there is less γ - Fe_4N needles in the substrate. The recrystallized dendrite-shaped upper ferrite layer retards the diffusion of the nascent atoms

and their penetration is cramped. In spite of that there are compound layer nuclei in the non-recrystallized areas of the electrolytic Fe like that in the untreated oxy-nitrocarburized electrolytic Fe.

The oxy-nitrocarburized structure of the vacuum annealed at 950°C electrolytic Fe and bulk Armco Fe (fig. 2c,d) shows differently shaped, sized and distributed nitrides. The finest needle-shaped nitrides in the electrolytic Fe probably are α'' -precipitates [9]. The α'' -crystal structure represents eight joined body-centred tetragonal lattices (Fe_8N or Fe_{16}N_2). α -Fe is in equilibrium with α'' under 400°C. The latter formation is facilitated due to the lattice resemblance. The α'' -nitrides contain less N atoms than γ' -ones. That's why α'' -precipitates are centred in the electrolyte Fe grains where the N concentration is less than at the boundaries. Consolidated γ' - Fe_4N are evident not only at the boundaries and near the surface but at the electrolyte-Armco Fe boundary where the nitrides coalesce because of the intensive N diffusion [10] and the defective structure. *Снимките са неподходящо изрязани!!!!*

The surface orientation of the Armco grains (fig. 2d) affects the γ' - Fe_4N growth. In this substrate γ' -nitrides development depends mainly on the N diffusion in the α -grains. Fe_4N grows up in {210} orientated grains in $\langle 100 \rangle$ direction [11]. Sometimes there are “lack of nitrides” areas at certain

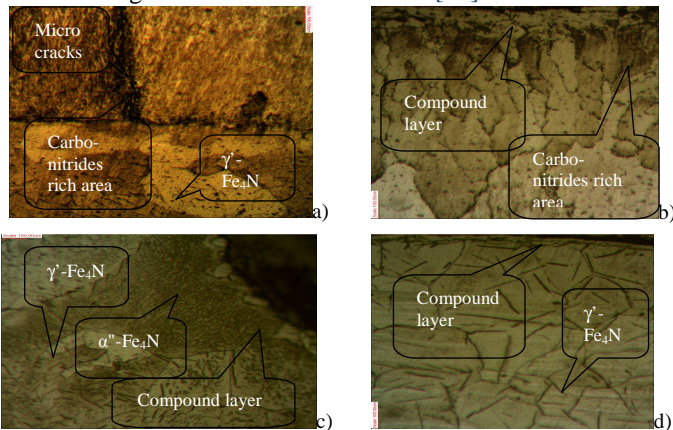


Fig.2 Microstructure images of the oxy-nitrocarburizing iron samples etched with Nital and Murakami reagent (500x): a) oxy-nitrocarburized untreated electrolytic Fe; b) oxy-nitrocarburized vacuum annealed electrolytic Fe at 600°C; c) vacuum annealed electrolytic Fe at 950°C; d) vacuum annealed Armco Fe at 950°C.

distances which are thought to be related with Z co-ordinate [12]. During full annealing and oxy-nitrocarburizing the α -grains release the excess C in form of boundary located Fe_3C . The latter renders the N diffusion and the γ' -needles morphology has changed. As the C concentration in α -Fe increases the N activity and thus decreases its solubility in the ferrite [3], this could be the reason for less nitride needles in Armco than in fully annealed electrolyte Fe. Consequently, the higher N and C surface concentration and the Fe_3C presence enhance a dense and integral compound layer formation. The spectral analysis shows a carbon concentration increase at an average of 0,035% in 0,1 mm depth.

3.2. XRD analysis for the non- and heat treated and oxy-nitrocarburized samples.

It is found that the traces of C, Mn, Si, Ni, etc. in the untreated Armco Fe and the oxides and other solid solutions in the vacuum annealed electrolytic Fe don't substantially change the α -Fe lattice parameters because there is a coincidence of the three α -phase diffraction peaks. The untreated electrolytic Fe peaks are shifted together and as a result, there is a total coincidence of the theoretical and experimental α -Fe parameters. There is symmetrically widening of the latter peaks which means fine grained and strained structure [13].

Fig.4 compares the X-ray diffraction patterns of the oxy-nitrocarburized samples. The quantity of Fe_4N is more than $\text{Fe}_{2,3}(\text{N,C})$ in the untreated oxy-nitrocarburized electrolytic Fe (fig. 4a). From thermodynamic point of view the Gibbs free energy for ultra fine grained material at 500°C is -8,22 kJ/mol for γ' - and -1,69 kJ/mol for ϵ -phase formation. A grate part of free energy is locked in this strained

structure in form of non-equilibrium defects that also push ahead the γ' -phase transformation. Each crystal reacts according to its size – the initial rate is higher because the smaller grains react first. The extent of the phase transformation depends on the grain size distribution [14]. As the fine grains predominate the quantity of the γ' -phase is greater. The activating energy for N diffusion through the boundaries is approximately half in comparison with crystal lattice diffusion [15]. An approval of the ϵ -phase carbo-nitride character is the decrease in c/a lattice parameters [16]. There is such a decrease in all of the treated samples but the calculated one is scarcely perceptible probably due to the low carbon potential in the gas phase. According to [17] the gas phase carbon potential should be high enough when Fe and low-carbon steels were nitrocarburized.

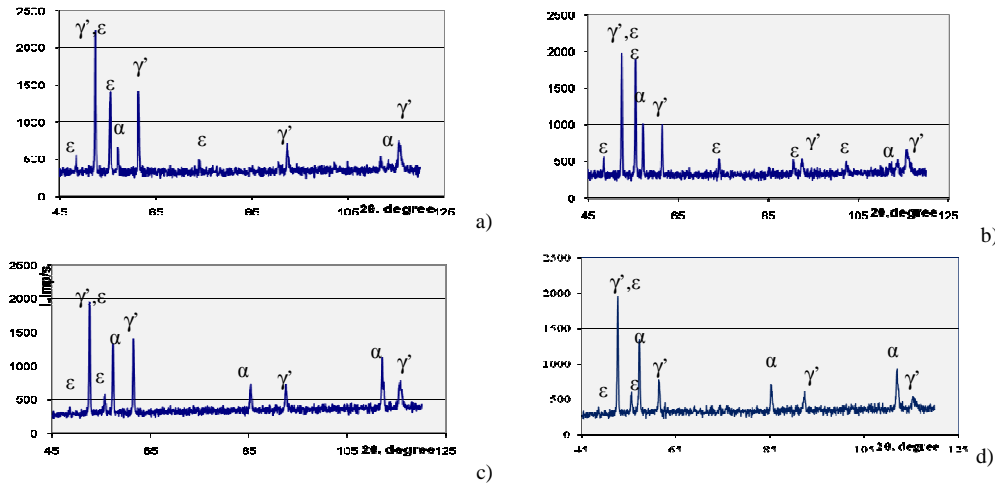


Fig.4 XRD pattern of oxy-nitrocarburized samples: a) oxy-nitrocarburized untreated electrolytic Fe; b) oxy-nitrocarburized vacuum annealed electrolytic Fe at 600°C; c) oxy-nitrocarburized vacuum annealed electrolytic Fe at 950°C; d) oxy-nitrocarburized annealed at 950 °C Armco Fe.

The content of ϵ -phase in the low temperature annealed electrolytic Fe (fig. 4b) is higher than that shown in fig.4a. In steels ϵ -Fe₂₋₃(N,C) forms easily from Fe₃C [18]. The ϵ -phase here is a result of a continuous increase in the surface N concentration and retard diffusion through the re-crystallized grains.

The X-ray diffraction pattern of the vacuum annealed at 950 °C electrolytic (fig. 4c) and Armco-Fe (fig. 4d) shows γ' -nitride prevalence in both of them. In the Armco-Fe sample except due to the continuous increase in the surface nitrogen concentration, ϵ -Fe₂₋₃(N,C) phase may be formed by means of Fe₃C transformation. The spectral analysis shows a carbon concentration increase at an average of 0,027% at the surface of the nitrocarburized Armco-Fe. The extension of some diffraction peaks probably corresponds with the strain field anisotropic character around the nitride precipitates and their predominant crystallographic orientation in the α -Fe matrix [13]. As a result of the uneven nitrides distribution in the three possible directions, a tetragonal distortion of α -phase occurs [19].

3.3 Cross-sectional hardness profile

The hardness of the diffusive layer (table 2) should be associated with the pre-saturation of the α -solution, nitrides' precipitation, compressive residual stress [20,21] and the initial hardness of the substrate. As it could be expected the increase in the hardness is not great because it is due to the fine but soft phases or

residual stress in the structure. The vacuum annealed at 950 °C electrolytic-Fe (fig. 5c) and Armco-Fe (fig. 5d) shows a gradual microhardness decrease. The fully annealed electrolytic-Fe microhardness remains slightly higher than the Armco-Fe one because of the smaller nitride phases. The pre-saturation of the α -Fe and low compressive stress determine the increase in the Armco-Fe hardness. The microhardness of the vacuum annealed at 600°C electrolytic-Fe at a distance of 150 μm from the compound zone towards the core slightly decrease and then maintains unchanged (fig.5b).

Table 2. Hardness values (HV_1) before and after oxy-nitrocarburizing.

Sample		Untreated	600°C	950°C
		[HV_1]	annealed [HV_1]	annealed [HV_1]
Before treatment	EL.-Fe	400	80	75
	Armco	130	125	120
After treatment	EL.-Fe	550	350	235
	Armco	-	-	205

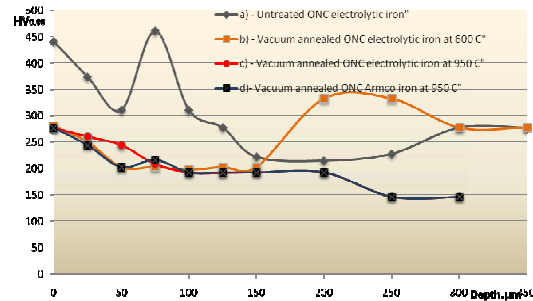


Fig.5 Comparison of the depth profile of the microhardness results of the vacuum oxynitrocarburized electrolytic and Armco-Fe without and after vacuum annealing.

These values corresponds to the **dendrite-like re-crystallized grains**. The underneath increase of the hardness is in the ultra fine, strained and nitrogen rich

electrolytic zone. The highest microhardness value belongs to the untreated oxy-nitrocarburized electrolytic-Fe (fig.5a). The fluctuation in the measurements is due to the partial relaxation of the IIIrd type structural stresses and the re-crystallization process near the surface as well as the nitrogen saturation in depth. The lack of coincidence in the maximum values of the untreated and annealed at 600°C Fe is due to the difference in electrolyte-Fe thickness and the position of the re-crystallized boundary in them.

4. Conclusion

The main conclusions from this investigation could be summarized as followed:

1. The structural characteristics of the substrate determine to a great extent the diffusion rate and the saturation depth of the vacuum ONC layers. *He zo razburam!*
2. According to the metallographic analysis, the C enriched areas appears in the ONC samples near to the surface, in some defective regions in the electrolyte-Fe and in the electrolyte - Armco Fe boundary where the nascent atoms decrease their diffusion rate. The diffusion of N is many times greater than the C one. In the oxy-nitrocarburized Armco Fe, the increased C content at a distance of 0,1 mm is due to C diffusion in the substrate.
3. It is found out that the ϵ -phase C content is comparatively low in the indicated process conditions.
4. The essential structural differences in the fully annealed electrolytic and Armco Fe compound and diffusion layer are shown. While the electrolytic Fe saturated zone contains a thinner ϵ - and γ' -built compound layer and α'' and γ' - constructed diffusion layer, the Armco shows a comparatively dense ϵ - and γ' -built compound layer and coarse γ' -nitride precipitates in the diffusion layer.
5. There is an inconsiderable hardness increase after treatment due to the pre-saturation of the α -Fe and compressive stress in the Armco substrate. The quantity and the dispersion of the nitride phases in the annealed samples contribute the hardness rise. In the untreated and low temperature annealed oxy-nitrocarburized samples there is an additional strength because of the residual stress in the structure.

Acknowledgements

The study was supported by contract № BG051PO001-3.3.04/28, "Support for the Scientific Staff Development in the Field of Engineering Research and Innovation". The project is funded with support from the Operational Programme "Human Resources Development" 2007-2013, financed by the European Social Fund of the European Union.

References

- [1] Bell T., Heat Treat. Met., 1975, 2(2), p.39–49;
- [2] Dawes C., Tranter DF, Reynoldson RW., Heattreatment'73; London, The Metals Society; 1973;
- [3] Winter Karl-Michael, Techn. Paper, Process-Electronic GmbH, United Process Controls, Heiningen, Germany;
- [4] Danev P., Ruse-University Scientific Proceedings, Ruse, 2004, p. 73-77, ISSN 1311-3321;
- [5] Горелкин СС., Расторгуев ЛН., Скаков ЮА., *Металлургия*, Москва 1970, 4;
- [6] Naumann FK., Langenscheid G., Arch. Eisenhüttenwes. 36, 1965, p.583-590;
- [7] Nikolova M, Danev P., Dermendjiev I, Metal 2010, 19 Int. Metal. Conference: Roznov pod Radhostem, May 2010, p 148;
- [8] Somers M. Proefschrift; Chem. Tech. and Mat. Sci. of the Delft University of Technology, 1989;
- [9] Maliska AM, de Oliveira AM., Klein AN, Muzart JLR, Surf. Coat. Technol., 141 (2001) 128-134;
- [10] Каратеев АМ., Павлюченко АА., Костик ЕА., Вост. – европейский Журнал Передовых Технологий – 4/1(16), 2005;
- [11] Inokuti Y., Nishida N., Oashi N, Metall. Trans. 6A (1975) 773-784;
- [12] Bernal JL., Salas O., Figueroa U., Oseguera J., Surf. Coat. Technol. 177-178 (2004) p.665-670;
- [13] Jung KS., Schacherl RE., Bischoff E., Mitemeijer EJ., Surf. Coat. Technol. 204 (2010) 1942-1946;
- [14] Pelka R., Arabczyk W., 2nd National Conference on Nanotechnology, NANO 2008;
- [15] Tong WP., Tao NR., Wang ZB., Lu J., Lu K., Sci, Vol 299, 203;
- [16] Naumann FK, Langenscheid, G. Arch Eisenhüttenw 1965; 36:677;
- [17] http://www.eltromoscau.narod.ru/karbon_oxid.htm;
- [18] Ratajski J., Surf Coat. Technol. 203 (2009);
- [19] Лахтин ЮМ., Коган ЯД., *Азотирование стали*, Москва, Машиностроение, 1976;
- [20] Bell T., Loh NI., Heat Treatment, 2, (1982) 232;
- [21] Priestner R., Priestner DM, Surf. Eng. 10 (1994) 65;